# Voltage-Controlled Slow Light via Resonant Tunneling Induced Transparency in Vertically aligned Conical Double Quantum Dot Molecules

Nooralhuda S.Yaqoob   and  Sabah M.M. Ameen*

Physics Dept., College of Science, University of Basrah, Basrah, Iraq.

* Corresponding author. Email: sabah.ameen@uobasrah.edu.iq

## Abstract

The electronic states of InAs/GaAs quantum dot has investigated for vertically-aligned double conical quantum dots molecule (CQDM). We calculated Eigen energies as a function of external voltage, wetting layer thickness and inter-dot spacer. Tunneling-induced transparency (TIT) in vertically coupled InAs/GaAs quantum dots using tunneling instead of pump laser, analogous to electromagnetically induced transparency (EIT) in atomic systems, has studied. The inter-dot quantum coupling strength is tuned by static electric fields. For parameters appropriate to a 100 Gbits/s optical network, slow down factor (SDF) as $10^9$ can be achieved. The scheme is expected to be useful to construct a variable semiconductor optical buffer based on TIT in vertically coupled InAs/GaAs quantum dots controlled by electric fields.

**Keywords:**  Quantum dot, Optical Buffer, Electronic states, Electromagnetically induced  transparency, Tunneling induced transparency, Slow light.

## 1. Introduction

Three-dimension confinement of charge carriers in the semiconductor structures have been extensively investigated due to their unique properties and vast variety of applications in different systems such as photonics and opto-electronic devices [1, 2], life sciences [3] and lasers [4]. Such structures can be fabricated using Stranski-Krastanov method in MBE and MOCVD [5]. In this technique, a few number of atomic layers of semiconductors like InAs are deposited on a substrate such as GaAs

[5, 6]. Due to lattice mismatch between the growing layer and the base material, the strain effects drives the quantum dots (QDs) towards 3D islands. The unconverted QD material is called wetting layer [5-7].

QDM is formed by coupling two neighbored QDs resulting in formation of electronics and optical states different from those of single QD [8]. Vertical and horizontal (lateral) coupling of QDs have been the subject of researches in the past decade [9-12]. Both vertical and horizontal coupled QDs have been proposed for applications in quantum information [13-15].

Since the random nature of self-assembly growth process leads to a size and location distribution of QDs ensemble [16], the investigation of distance-dependent electronic and optical properties of QDs in a QDM is of great importance. The distance between QDs in a QDM –so called herein "interdot spacer" has been proved to play an important role in coupling degree of QDs in a QDM [14, 17]. Barticevic *et. al*. [17] proposed a theoretical study of electronic and optical properties of laterally coupled quantum dots under a magnetic field perpendicular to the plane of dots. Bayer *et. al*. [14] studied the emission of an interacting electron-hole pair in a single QDM as a function of spacer.

Extensive theoretical studies of the electronic and optical properties of QDs have been performed by several groups [18–22]. However, no theoretical studies of the electron tunneling rate for conical quantum dots of real geometry have been reported to date. In light of the promising IR detector application of QD systems, it is desirable to investigate the electron tunneling rate, so that the dark current of the QD device can be assessed.

Slow light phenomena have potential applications such as optical communication (all optical buffers, ultrasensitive switches) [23], nonlinear optics with low optical intensity, and quantum information storage [24]. The design of slow light devices using semiconductor nanostructures is of great interest because the use of semiconductor components have widespread in optoelectronics and these devices can be potentially integrated with other components in an optical communication systems. The "quantum dot molecule" QDM consisting of a vertically stacked pair of

InAs/GaAs islands formed via strain driven self-assembly is a promising system for communication. Recently, inter-dot coupling controlled by applying an external electric field in an individual QDM was observed [25]. All-optical logic gates based on QDs seem to be the essential element in ultrahigh speed networks which can perform many important functionalities. The speed of all-optical switches is determined by the carrier dynamics. The fast carrier relaxation between QD states could be utilized to enhance the device speed and switching performance. Various schemes of all-optical logic gates like XOR operation are usually limited to 100 Gb/s due to the long carrier life time in the QD. It has been shown that the dual semiconductor optical amplifier SOA based on quantum dots is a promising method for the realization of high-speed all-optical logic systems in the future [26-28].

Due to the geometrical complexity, a numerical method of finite element has been adopted to solve Schrodinger's equation with strained potential. The calculations are done by using "COMSOL" framework and homemade MATLAB codes. Energy eigenvalues has been calculated as a function of each of the following parameters: external voltage, wetting layer and QDM spacer where other parameters of a single conical-shaped are held constant. The maximum obtainable slow down factor (SDF) (which it is a measure of the group-velocity reduction), was examined. The SDF is a figure of merit relevant for optical storage. In this paper, we investigate the vertically aligned conical QDM system as an optical buffer for application to 100 Gbps optical communication systems. We use proper parameters of strained QDs from our electronic band structure model using COMSOL Multiphysics software and homemade Matlab codes for estimating SDF.

## 2. The Method

In this paper, the confined electronic states of the self-assembled InAs/GaAs vertically-aligned conical QDM structures with wetting layer are obtained through solving the stationary state Schrödinger equation. SDF is calculated with the help of density matrix theorem.

## 2.1 The electronic structure

The wave functions and energy eigenstates of electrons and holes in conical QDM were determined through one band Schrodinger's equation in effective mass approximation:

$$-\nabla \cdot \left( \frac{h^2}{8\pi^2 m^*} \nabla\psi(r) \right) + V(r)\psi(r) = E\,\psi(r), \tag{1}$$

where $h$ is Planck's constant, $m^*$ is the effective mass, $V(r)$ is the potential energy, $E$ is the energy eigenvalue, $\psi$ is the quantum mechanical wave function. Since the conical QDM with wetting layer (WL) is rotationally symmetric, the problem has been reduced to a two dimensional one. Hence, the wave function can be written as

$$\psi(r) = \phi(r, z)\, e^{il\varphi}, \tag{2}$$

where $l = 0, \pm 1, \pm 2, \dots$ is the orbital quantum number obtained by applying the periodic boundary condition. Then the Schrödinger's equation in the cylindrical coordinates has the form:

$$-\frac{\hbar^2}{2m^*} \left( \frac{1}{r}\frac{\partial}{\partial r}\left( r\,\frac{\partial}{\partial r}\right) + \frac{\partial^2}{\partial z^2} - \frac{l^2}{r^2} \right) \phi_l(r,z) + V(r,z)\,\phi_l(r,z) = E_l\,\phi_l(r,z), \tag{3}$$

where $\phi_l$ is the envelope wave function. In order to solve Eq. (3), it must be transformed to a generalized form of a coefficient partial differential equation used by COMSOL as:

$$\nabla.(-c\nabla u - \alpha u + \gamma) + au + \boldsymbol{\beta}.\nabla = d_a\lambda\,, \tag{4}$$

where $d_a$ is a damping coefficient or mass coefficient, $c$ is the diffusion coefficient, $\alpha$ is the conservative flux convection coefficient, $\boldsymbol{\beta}$ is the convection coefficient, $a$ is the absorption coefficient and $\gamma$ is the conservative flux source term. The non-zero coefficients are [29]:

$$c = \frac{h^2}{(8\pi^2 m_e^*)}, \quad a = \left[\frac{h^2}{8\pi^2 m_e^*}\right]\frac{l^2}{r^2} + V - V_a * \frac{z}{L}, \quad \beta_r = \left(\frac{-h^2}{8\pi^2 m_e^*}\right) * \frac{l}{r}, \quad d_a = 1 \text{ and } \lambda = E_l. \tag{5}$$

The Comsol overall axisymmetric 2D structure is shown in Fig. 1 below, where "$d$" is the wetting layer thickness, "$R$" is the radius and "$H$" is the QD height and $L$ is the overall vertical length of the structure as indicated in Fig. 1. Indeed, Eq. (3) is solved for $l$=0. To resolve this problem, we use the form PDE Comsol interface

coefficient, where the system structure was solved for eigenvalue/eigenvector model. Electron volt is used as an energy and nanometer as a length units of the geometry. We can model the overall structure in 2D as shown in Fig. 1

## 2.2 Susceptibility of conical QDM

The electronic band structure of the conical QDM system is sketched as in Fig. 2. Consider the significant interdot tunneling matrix element $T_e \equiv T_{12}$ is between the first and second conduction band states in the above and lower QD, respectively and neglecting hole tunneling, the total Hamiltonian of the system is [30]:

$$H = E_o|0\rangle\langle0| + E_1|1\rangle\langle1| + E_2|2\rangle\langle2| + T_e|1\rangle\langle2| +$$

$$\hbar\Omega_s \, exp(i\omega_s t)\,|0\rangle\langle1| + h.c, \tag{6}$$

where $E_i = \hbar\omega_i$ $(i = 0, 1, 2)$ is the energy of state $\langle i|$, $T_e$ is the tunneling coupling, $\omega_s$ is the signal laser frequency, and $\Omega_s = \mu E/2\hbar$ is the optical coupling with $\mu$ dipole momentum matrix element and $E$ is the signal electric field amplitude.
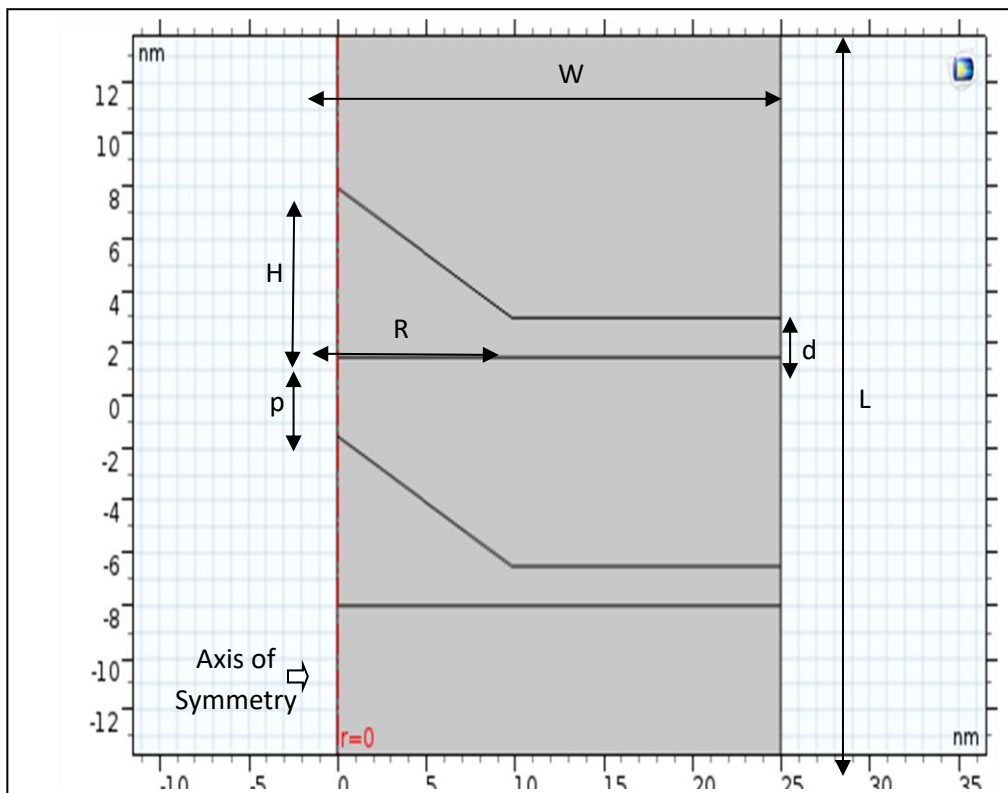


**Fig. 1** Two dimensional geometry of axisymmetric conical QDM with wetting layer.
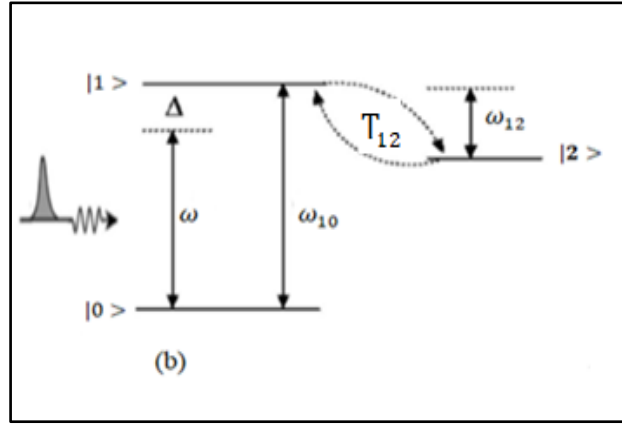
**Fig. 2** The electronic band structure of the three level system.

One can get the complete set of coupled differential equations for the density matrix $\rho_{ij}$ elements by using the Liouville–Von Neumman–Lindblad equation:

$$\dot{\rho} = \frac{-i}{\hbar}[H, \rho] + \mathcal{L}(\rho),$$  (7)

where $\rho$ is the density matrix operator, $H$ is the three-level system Hamiltonian, and $\mathcal{L}(\rho)$ represents the Liouville operator describing the decoherence processes

$$\mathcal{L}(\rho) = \frac{1}{2}\sum_i \begin{bmatrix} \Gamma_i^j(2|j\rangle\langle i|\rho|i\rangle\langle j| - \rho|i\rangle\langle i| - |i\rangle\langle i|\rho) + \\ \gamma_i(2|i\rangle\langle i|\rho|i\rangle\langle i| - \rho|i\rangle\langle i| - |i\rangle\langle i|\rho), \end{bmatrix}$$  (8)

where $\Gamma_i^j$ is the decaying rate from the state $|i\rangle$ to the state $\langle j|$ and $\gamma_i$ is the pure dephasing rate. With Eq.'s (6), (7) and (8), one can get the complete set of coupled differential equations for the density matrix $\rho_{ij}$ elements as follows:

$$\dot{\rho}_{10} = -i\left((\omega_{10} + \gamma_{10})\rho_{10} + \Omega_s e^{-i\omega_s t}(\rho_{11} - \rho_{00}) + T_e\rho_{20}\right)$$  (9.a)

$$\dot{\rho}_{12} = -i\left((\omega_{12} + \gamma_{12})\rho_{12} + (\rho_{22} - \rho_{11})T_e - \Omega_s e^{-i\omega_s t}\rho_{02}\right)$$  (9.b)

$$\dot{\rho}_{20} = -i\left((\omega_{20} + \gamma_{20})\rho_{20} + T_e\rho_{10} + \rho_{21}\Omega_s e^{-i\omega_s t}\right)$$  (9.c)

From Eq. (9), one can get

$$\dot{\tilde{\rho}}_{10} = -(\gamma_{10} + i\Delta_s)\tilde{\rho}_{10} - i\Omega_s(\rho_{11} - \rho_{00}) + iT_e\tilde{\rho}_{20}$$  (10.a)

$$\dot{\tilde{\rho}}_{12} = -(\gamma_{10} + i\Delta_s)\tilde{\rho}_{12} + \frac{i}{\hbar}T_e(\rho_{22} - \rho_{11}) - i\Omega_s^*\tilde{\rho}_{02}$$  (10.b)

$$\dot{\tilde{\rho}}_{20} = -(\gamma_{20} + i\Delta_s)\tilde{\rho}_{20} + \frac{i}{\hbar}(T_e + \Omega_s^*)\tilde{\rho}_{10} - i\Omega_s^*\tilde{\rho}_{21}$$  (10.c)

where $\Delta_s = \omega_{10} - \omega_s$ is detuning from the signal beam. As the QDM system is initially in the ground state $|0\rangle$, therefore, $\rho_{00}^{(0)} = 1$ and $\rho_{11}^{(0)} = \rho_{22}^{(0)} = \rho_{21}^{(0)} = 0$. The set of equations can be solved for the above initial conditions, so $\rho_{10}$ is:

$$\tilde{\rho}_{10}(t) = \frac{i\Omega_s(\rho_{11}-\rho_{00})}{\tilde{\gamma}_{10}\left[1+\frac{(Te+\Omega_s)^2}{\tilde{\gamma}_{20}\tilde{\gamma}_{10}}\right]},\tag{11}$$

where $\tilde{\gamma}_{10} = (\gamma_{10} + i\Delta_s)$ and $\tilde{\gamma}_{20} = (\gamma_{20} + i\Delta_s)$. Hence, the complex susceptibility of the QDM is:

$$\chi = \frac{\Gamma_{opt}}{V}\frac{|\mu|^2}{\varepsilon_0\hbar\Omega_s}\tilde{\rho}_{10},\tag{12}$$

where $\Gamma_{opt}$ is the optical confinement factor, $V$ is the physical volume of the single QD. So, the complex permittivity can be written as:

$$\mathcal{E}_1 = \mathcal{E}_{bac} + \chi = n_{bac}^2 + U\frac{i\Omega_s(\rho_{11}-\rho_{00})}{\tilde{\gamma}_{10}\left[1+\frac{T_e^2}{\tilde{\gamma}_{20}\tilde{\gamma}_{10}}\right]},\tag{13}$$

where $U = \frac{\Gamma}{V}\frac{|\mu|^2}{\varepsilon_0\hbar}$. Since, $\chi$ is very small, we can determine the light group velocity according to $v_g = c/[n + \omega(dn/d\omega)]$, where $n \approx 1 + 2\pi\chi$ and then[25]:

$$c/v_g = 1 + 2\pi Re\chi(\omega)|_{\omega=\omega_{10}} + 2\pi Re(d\chi/d\omega)|_{\omega=\omega_{10}}\tag{14}$$

when $Re\{\chi(\omega)\}_{\omega=\omega_{10}}$ is zero and the dispersion is very steep and positive, the group velocity is reduced, and then $c/v_g = 1 + 2\pi Re\{d\chi/d\omega\}_{\omega=\omega_{10}}$ [30]. The group velocity SDF is defined as the ratio of the light propagation time of the device length to that of free space. When the detuning from the signal beams are zero, the SDF at the signal frequency $\omega_s$ can be derived from this dielectric constant.

$$SDF = \left[\frac{\varepsilon_{bac}+\sqrt{\varepsilon_{bac}^2+\varepsilon_{res}^2}}{2}\right]^{\frac{1}{2}}\left[1+\frac{\hbar\omega_s}{2\sqrt{\varepsilon_{bac}^2+\varepsilon_{res}^2}}\frac{U_{10}(T_e^2-\gamma_{20}^2)}{\hbar^2(\gamma_{20}\gamma_{10}+T_e^2)^2}\right]\tag{15}$$

## 3. Results and Discussion

### 3.1 The effect of inter-dot spacer

We examine the coupling between the dots as an example of a vertically aligned array of two coupled quantum dots with wetting layers of thickness 1.3 nm. A few different interdot spacers in the range of 1.5-5 nm were selected. Fig. 3 shows the dependence of the confined energy levels on the spacer. We notice for a large QD separation the lower two energy levels of the QDM system approach those of a single QD, with the difference that each level is doubled. This process is present, however, much slower also for the higher eigenvalues, which means that the higher excited states easier become coupled also at larger distances. Accordingly, the figure show, when the spacer is small, the coupled QDM behave like a double potential well and the envelope functions are similar of ground and first excited states of a single QD. With increasing the spacer, the mutual interaction between the dots becomes weaker and the dots are uncoupled. In this situation the dots act as single QDs and the far QD energy eigenvalues of ground and first excited states tend to be coincide on ground state energy of a single QD.
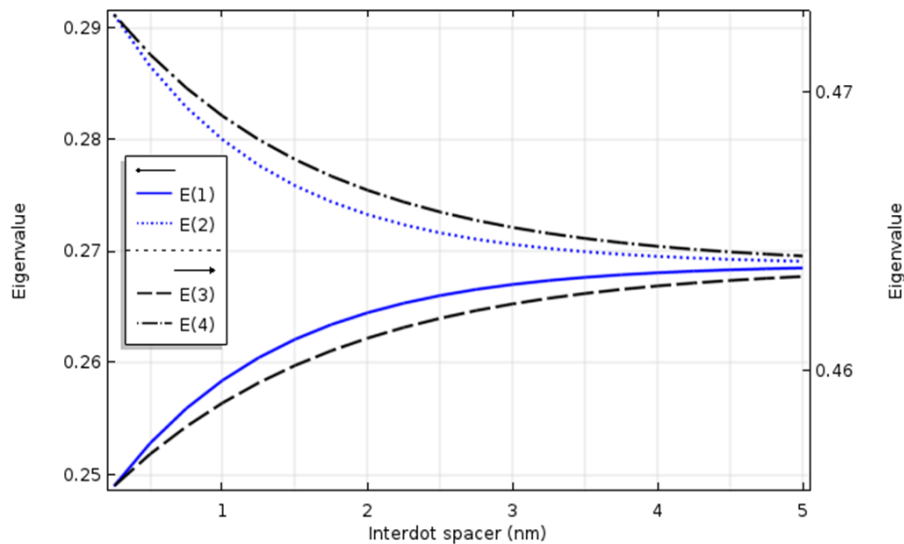


**Fig. 3** The first four Energy eigenvalues of electrons in the C.B as a function of QD spacer.

## 3.2 The effect of wetting layer

We have made changes to the wetting layer thickness of the conical QDM applied within the range (0.1-1.5) nm. The energy eigenvalues are shown in Fig. 4. We have observed the electron wave functions superposition in the vertically grown coupled conical shape quantum dots. The wave functions for the ground state and the first excited of InAs/GaAs QDs with and without WL have been calculated and presented. In Fig. 5, an envelope function is shown corresponding to a state where coupling between the wetting-layer region and the quantum-dot region exists, although the coupling is relatively weak. Moreover in presence of wetting layer, part of the envelope wave function extends into the wetting layer but the general localization does changes.
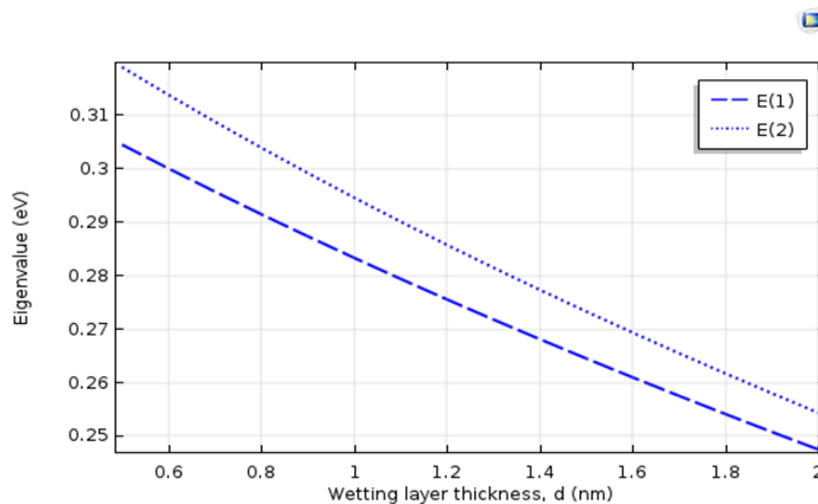


**Fig. 4** The first two Energy eigenvalues of electrons as a function of wetting layer thickness.

## 3.3 The effect of external voltage

The external electric field applied on quantum dot structure changes their potential profile and, therefore, level positions therein. The symmetric QD in presence of an electric field becomes asymmetrical, and the wide rectangular QD can be transformed to triangular one with changing the corresponding energy spectrum [31]. A considerable attention the calculation of a level position in QD structure under external electric field was carried out with the help of a procedure [30]. Therefore, Utilization of external voltage tilts the wells potential and decreasing their

conjugation strength and modifies the group velocity. We have made changes to the external voltage values of the double conical quantum points applied within the range (1-4) eV as shown in Fig. 6.
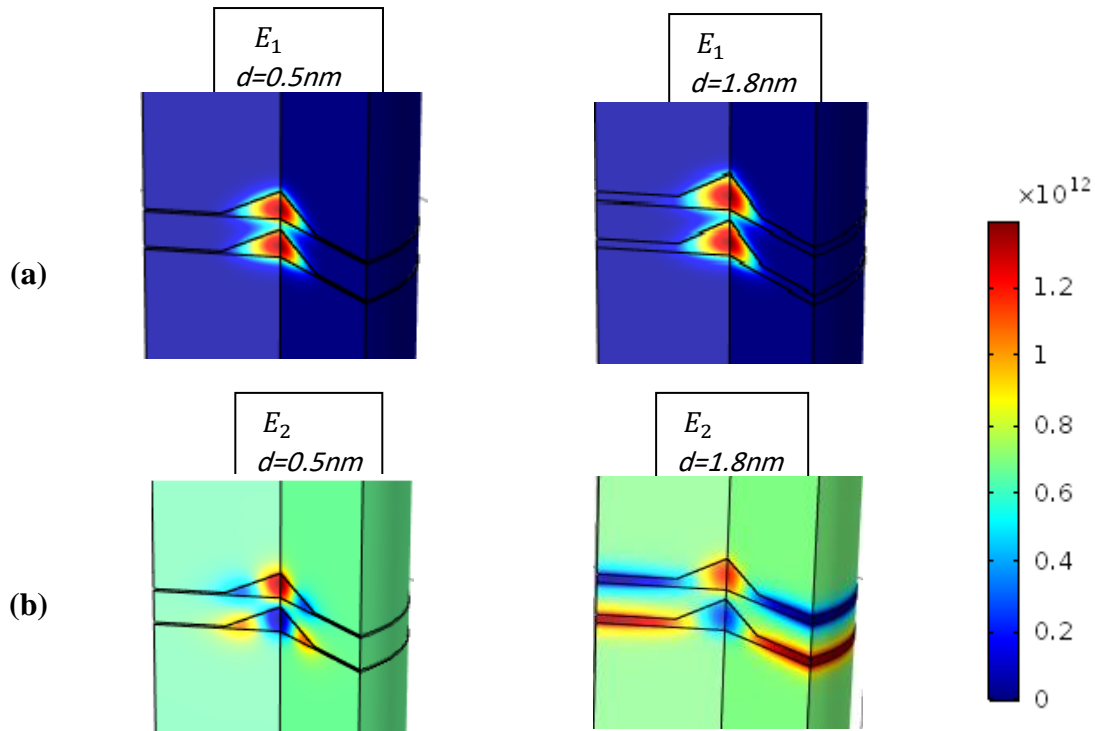


**Fig. 5** Envelope wave functions of CQDM. **(a)** The ground-state, **(b)** The first excited state.

In the presence of external electric field a considered symmetrical QDM becomes asymmetrical, and furthermore triangular if the electric field is strong and the energy of a bound state reduced with increasing field as long as the energy level remains in quadrangular region of the well (see fig. 7). In strong electrical fields the energy level is transferred into triangular region of the well.

In Fig. 7, we choose two cases to describe the effect of external applied voltage on the envelope wave functions. The first one is at 2.0 eV where the tunneling is still at low levels while the second one is at 3.45 eV at which the tunneling takes its maximum value where the energy levels of the two QDs are nearly coincident.
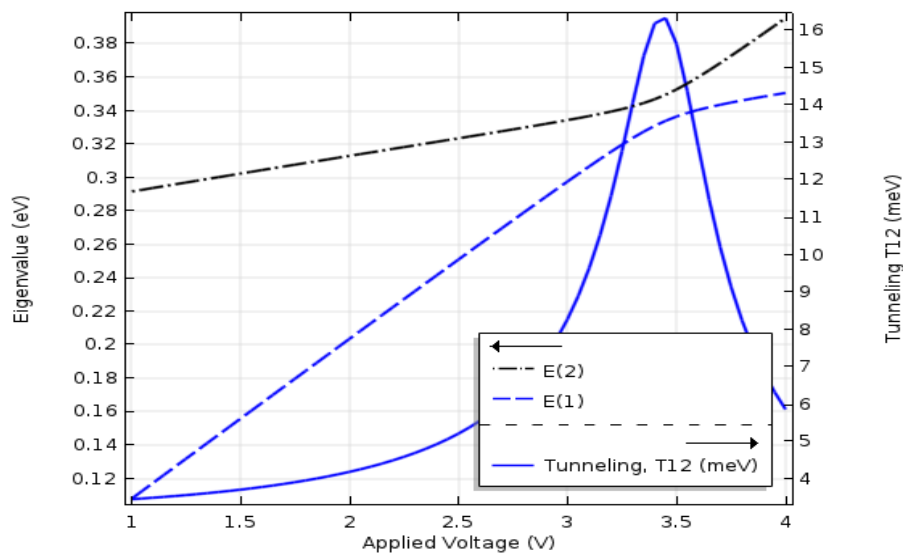
**Fig. 6** The tunneling and eigenvalues as a function of the external voltage.

## 3.4 Tunneling matrix elements

Bardeen's theory viewed the tunneling current as the net effect of many independent scattering events that transfer electrons across the tunneling barrier [31]. With adequate knowledge of the electronic state of the sample and the tip, one can approximate the rates of these individual scattering events, and arrive at an expression for the tunneling current: it equals the net rate of transfer of electrons between tip and sample multiplied by the charge of an electron. Bardeen's tunneling theory (upon Duke's interpretation) is based on several assumptions [31, 32]. The tunneling matrix elements can be found via an integral over a surface in the barrier region lying between the QDs [32]:

$$T_{mn} = -\frac{\hbar^2}{2m^*} \int \left( \psi_n^* \frac{\partial \psi_m}{\partial z} - \psi_m \frac{\partial \psi_n^*}{\partial z} \right) ds, \tag{16}$$

where $m^*$ is the effective mass of the electron, $\psi_m$ and $\psi_n$ are the envelope wave functions corresponding to states $m$ and $n$ respectively where the tunneling occurs between them. The integration is over the surface $s$ between the dots and normal to $z$ axis. We used Comsol to calculate the tunneling $T_{nm}$ and we got the results shown in the Table (1).
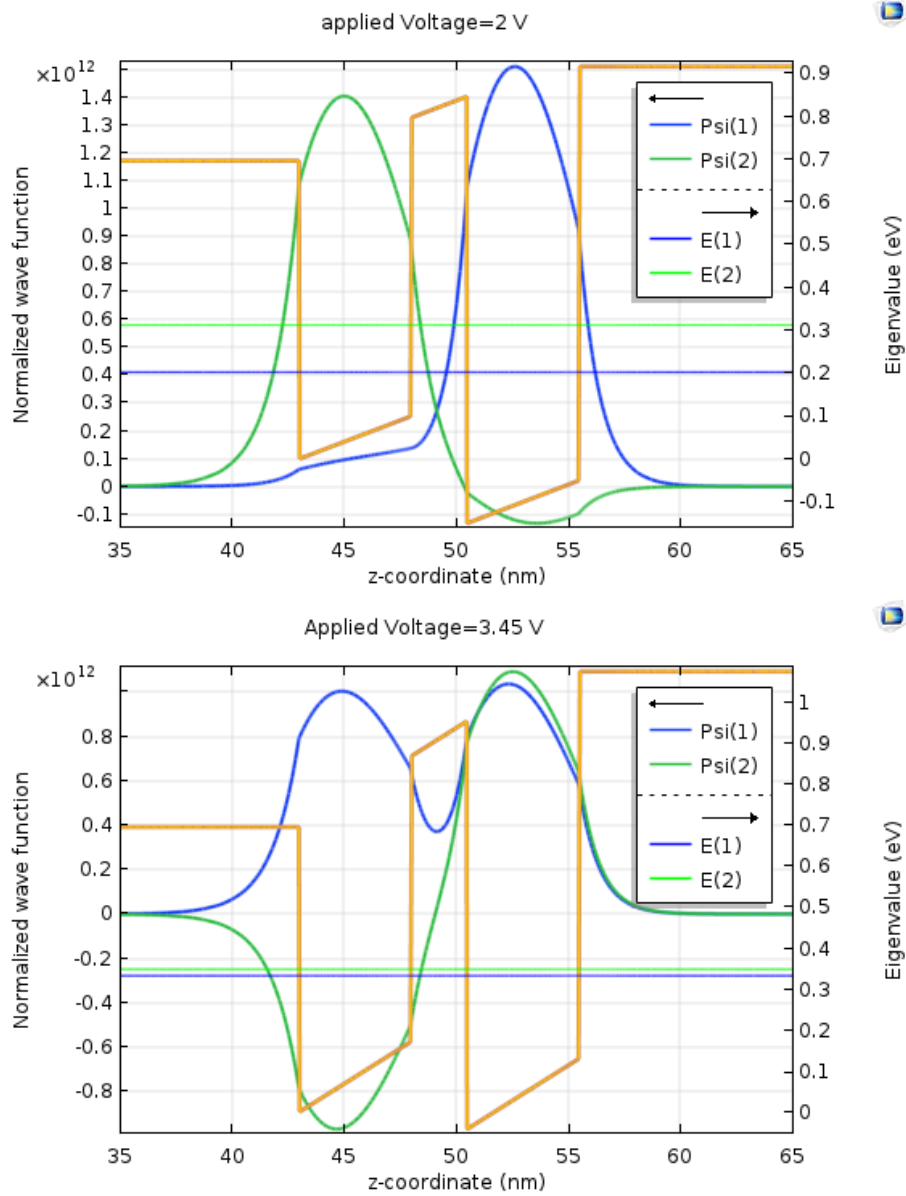
**Fig. 7** Wave function of the conical QDM at voltages of 2V and 3.45 V.

## 3.4 The SDF

We first investigate the spectral features of the slowdown factor and the spectral width over which slowdown can be achieved. To this end, we solve the dynamical equations for the steady-state value of the signal cw field.

The inter-band dipole moment $\mu_{10} = \langle \emptyset_{d1}(r)|ez|\emptyset_{d0}(r)\rangle$ has been calculated as a function of applied voltage to investigate the SDF at different linewidths $\gamma_{10}$. Results is listed in Table (1). And By using Eq. (13-15) we calculated the normalized refractive index, absorption spectra from the linear susceptibility and the SDF of the signal laser beam when the tunneling is varied via gate voltage, i.e., considering only external voltage (TIT method). The result of the normalized refractive index, absorption spectra are shown in Fig. 8 for different values of tunneling. An increased tunneling leads to a larger separation of the Autler-Townes resonances and a reduction of the slowdown factor S.

**Table 1**. Inter-band dipole moment for R=11.3 nm and d=1 nm at different external voltages.

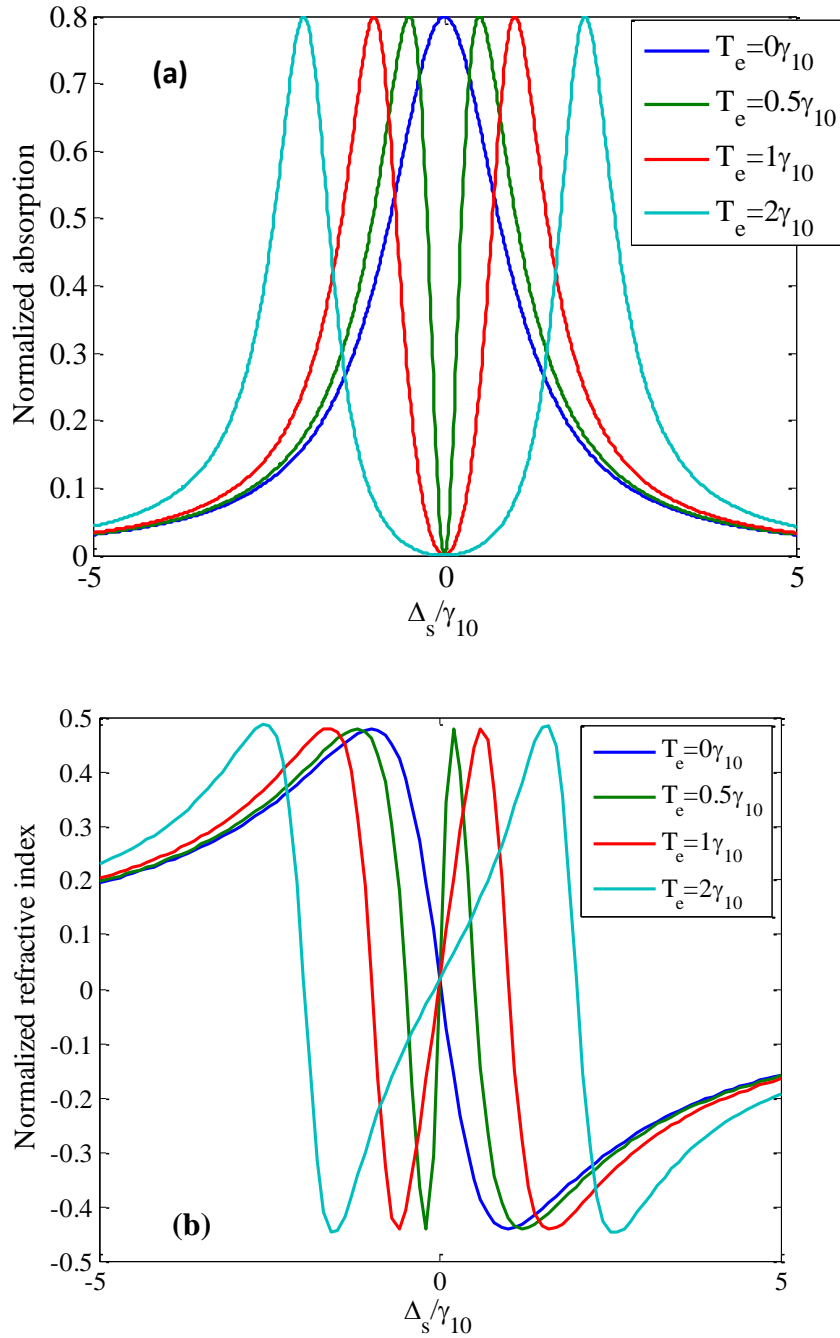| $V_a$ (eV) | $T_e$ (meV) | $\mu_{10}/e$ (Å) |
|---|---|---|
| 1.00 | 3.46 | 35.1 |
| 1.25 | 3.57 | 18.3 |
| 1.50 | 3.91 | 2.6 |
| 1.75 | 4.19 | 15.8 |
| 2.00 | 4.26 | 47.5 |
| 2.25 | 4.59 | 184.7 |
| 2.50 | 5.21 | 328.5 |
| 2.75 | 6.25 | 328.8 |
| 3.00 | 8.27 | 320.5 |
| 3.25 | 12.77 | 287.7 |
| 3.50 | 15.64 | 148.6 |
| 3.75 | 9.14 | 19.2 |
| 4.00 | 4.65 | 37.1 |

**Fig. 8** The dimensionless linear susceptibility as a function of normalized detuning $\Delta_s / \gamma_{10}$.
(a) the imaginary part, and (b) real part.

In Fig. 8 we display linear susceptibility as a function signal detuning for different values of tunneling. It is shown when the photon energy approximates the resonance energy of each QD, there is large anomalous dispersion which corresponds to superluminal propagation with high absorption peak. When the signal energy is just lied in the middle of the two QDs resonance energies, the bandwidth of transparency

window becomes wider with increasing the tunneling rate. Therefore, we can get a large bandwidth with small dispersion and subluminal propagation at zero detuning.
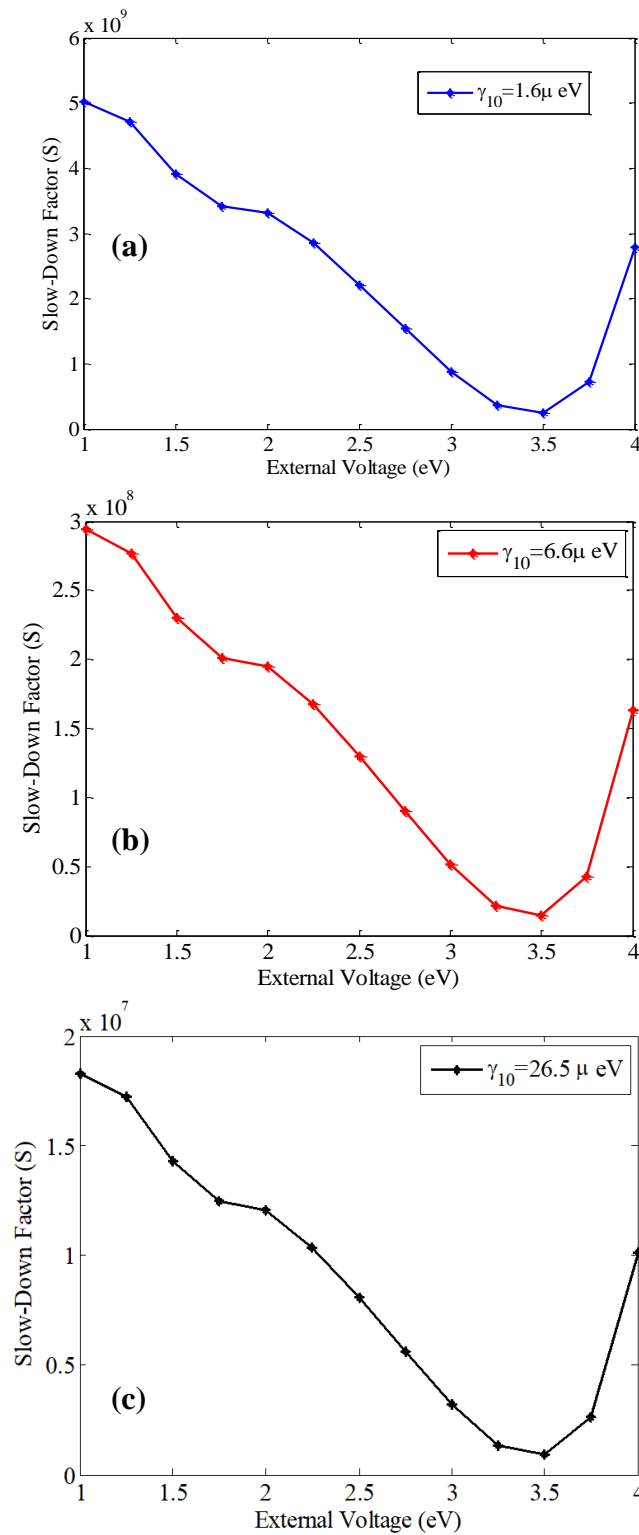


**Fig. 9** The group velocity SDF as a function of the external voltage at **(a)** $\gamma_{10} = 1.6\,\mu\,eV$, **(b)** $\gamma_{10} = 6.6\,\mu\,eV$, and **(c)** $\gamma_{10} = 26.5\,\mu\,eV$.

While Fig. 9 shows the SDF as a function of applied voltage at different values of linewidths. Based on the obtained results, it can be said when the applied voltage increased, the slope of real part of refractive index curve decreases and therefore, a smaller SDF is guaranteed with large bandwidth. It can be concluded that the SDF decreases with increasing the external voltages or $\gamma_{10}$, where about $10^9$ SDF can be obtained using conical QD system compared with $10^8$ using disk QD system [25].

The effect of the applied external voltage on the SDF (or group index) is investigated in this section. The largest group index is usually occurs for the frequencies of maximum absorption which makes these regions to be less important for applications. At a zero detuning frequency, big cancellation of absorption is showed, making it the frequency of choice for light slowing applications.

## 4. Conclusions

We used the one-band effective mass model for computation of electronic states in the conduction band. Our simulations showed that the wetting layer lowers the energy levels and therefore, an additional confined states can be introduced. Starting from the quasi analytic QD model, we constructed the states of the QDM and used these as input in the equations of motion of density matrix. Choosing probe fields and TIT for a $\Lambda$ scheme consisting of the three localized electron levels, we found SDF of the QDM that are far better than results achieved in single QDs. The absorption peak and transparency window bandwidth can be tuned by the applied electric field which control the tunneling as shown in Fig. (8). In our model, with $T_e$= 3.46 meV, we can get SDF of about $10^9$ at $\gamma_{10} = 1.6\ \mu\ eV$. Such a system may be applied in all optical buffers, optical switching and filters.

## References

[1]    A. Karimkhani, M. K. Moravvej-Farshi, Temperature dependence of optical near-field energy transfer rate between two quantum dots in nanophotonic devices. Applied Optics, 49 (2010) 1012-1019.

[2]   M. Heiss, Y. Fontana, A. Gustafsson, G. Wüst, C. Magen, D. O'Regan, Self-assembled quantum dots in a nanowire system for quantum photonics. Nature Materials, 12 (2013) 439-444.

[3]   T. Jamieson, R. Bakhshi, D. Petrova, R. Pocock, M. Imani, A. M. Seifalian, Biological applications of quantum dots. Biomaterials, 28 (2007) 4717-4732.

[4]   O. Karni, A. Capua, G. Eisenstein, D. Franke, J. Kreissl, H. Kuenzel, Nonlinear pulse propagation in a quantum dot laser. Optics Express, 21 (2013) 5715-5736.

[5]   M. Sabaeian, A. Khaledi-Nasab, Size-dependent intersubband optical properties of dome-shaped InAs/GaAs quantum dots with wetting layer. Applied Optics, 51 (2012) 4176-4185.

[6]   R. Melnik, M. Willatzen, Band structures of conical quantum dots with wetting layers. Nanotechnology, 15 (2004) 1-8.

[7]   A. Baskaran, P. Smereka, Mechanisms of Stranski-Krastanov growth, Journal of Applied Physics, 111 (2011) 044321.

[8]   H. Qin, A. Holleitner, K. Eberl, R. Blick, Coherent superposition of photon-and phonon-assisted tunneling in coupled quantum dots, Physical Review B, 64 (2001) 241302.

[9] M. Heldmaier, M. Seible, C. Hermannstädter, M. Witzany, R. Roßbach, M. Jetter, Excited-state spectroscopy of single lateral self-assembled In GaAs quantum dot molecules, Physical Review B, 85 (2012) 115304.

[10] M. Raith, P. Stano, F. Baruffa, J. Fabian, Theory of Spin Relaxation in Two-Electron Lateral Coupled Quantum Dots, Physical Review Letters, 108 (2012) 246602.

[11] Z. Liu, L. Wang, K. Shen, Energy spectra of three electrons in Si/SiGe single and vertically coupled double quantum dots, Physical Review B, 85 (2012) 045311.

[12] W. Gutiérrez, J. H. Marin, I. D. Mikhailov, Charge transfer magnetoexciton formation at vertically coupled quantum dots, Nanoscale research letters, 7 (2012) 1-6.

[13] C. Hermannstadter, M. Witzany, M. Heldmaier, R. Hafenbrak, K. Jons, G. Beirne, Polarization anisotropic luminescence of tunable single lateral quantum dot molecules, Journal of Applied Physics, 111 (2012) 063526.

[14] M. Bayer, P. Hawrylak, K. Hinzer, S. Fafard, M. Korkusinski, Z. Wasilewski, Coupling and entangling of quantum states in quantum dot molecules, Science, 291 (2001) 451-453.

[15] S. Yang, A. Bayat, S. Bose, Spin-state transfer in laterally coupled quantum-dot chains with disorders, Physical Review A, 82 (2010) 022336.

[16] B. Liang, P. Wong, N. Pavarelli, J. Tatebayashi, T. Ochalski, G. Huyet, Lateral interdot carrier transfer in an InAs quantum dot cluster grown on a pyramidal GaAs surface, Nanotechnology, 22 (2011) 055706.

[17] Z. Barticevic, M. Pacheco, C. Duque, L. Oliveira, A theoretical study of exciton energy levels in laterally coupled quantum dots, Journal of Physics: Condensed Matter, 21 (2009) 405801.

[18] M. A. Cusack, P. R. Briddon, M. Jaros, Electronic structure of InAs/GaAs self-assembled quantum dots, Phys. Rev. B, 54 (1996) 2300.

[19] K. Chang, J. B. Xia, Band parameters for nitrogen-containing semiconductors, Solid State Common., 104 (1997) 351.

[20] S. S. Li, J. B. Xia, Electronic and structural anomalies in lead chalcogenides, Phys. Rev. B, 55 (1997) 605-610.

[21] S. M. Komirenko, K. W. Kim, M. A. Stroscio, M. Dutta, Dispersion of polar optical phonons in wurtzite quantum wells, Phys. Rev. B, 59 (1999)  5013-5020.

[22] F. H. Fu, L. W. Wang, A. Zunger, Many-body pseudopotential theory of excitons in InP and CdSe quantum dots, Phys. Rev. B, 60 (1999) 1819-1829.

[23] C. J. Chang-Hasnain, P. C. Ku, J. Kim, S. L. Chuang, Variable Optical Buffer Using Slow Light in Semiconductor Nanostructures, Proc. IEEE, 91 (2003) 1884-1897.

[24] M. Fleischhauer M. D. Lukin, Dark-State Polaritons in Electromagnetically Induced Transparency, Phys. Rev. Lett., 84 (2000) 1-4.

[25] C. Yuan, K. Zhu, Y. Jiang, Voltage-controlled slow light in asymmetry double quantum dots, Appl. Phys. Lett., 89 (2006) 052115.

[26] X. Zhang, S. Thapa, N. Dutta, All-optical XOR gates based on dual semiconductor optical amplifiers, Cogent Physics, 6 (2019) 1660495.

[27] H. G. Yousefabad, S. Matloub, A. Rostami, Ultra-broadband Optical Gain Engineering in Solution-processed QD-SOA Based on Superimposed Quantum Structure, Nature Scientific Reports, 9 (2019) 12919.

[28] P. N. Goki, M. Imran, C. Porzi, V. Toccafondo, F. Fresi, F. Cavaliere, L. Potì, Lossless WDM PON Photonic Integrated Receivers Including SOAs, Appl. Sci., 9 (2019) 2457.

[29] COMSOL Multiphysics Model Library copyright 1998-2008 by COMSOL AB.

[30] C. Yu, H. Huang, L. Zhang, D. Xu, 'Double tunneling induced transparency in the asymmetry quantum dot molecules, Optica Applicata, 3 (2016) 474- 481.

[31] A. D. Gottlieb, L. Wesoloski, Bardeen's tunneling theory as applied to scanning tunneling microscopy: a technical guide to the traditional interpretation, Nanotechnology, 17 (2006) 1-22.

[32] M. Sahari, M. R. Mehmannavaz, H. Sattari, Optically controllable switch for light propagation based on triple coupled quantum dots, App. Optics, 11 (2014) 2375-2383.

السيطرة على ابطاء الضوء بالفولتية عن طريق الشفافية المستحثة نفقيا في جزيئة النقطة الكمية المخروطية
المزدوجة المرتية رأسيا

نور الهدى سعيد يعقوب        و        د. صباح مهدي محمدأمين

قسم الفيزياء، كلية العلوم، جامعة البصرة، البصرة، العراق

**المستخلص**

درست الحالات اللالكترونية لجزيئة النقطة الكمية InAs/GaAs المخروطية الشكل المتكونة من زوج من
النقاط الكمية المرتبة عموديا. حسبت مستويات الطاقة كدالة للجهد المسلط على النظام وسمك المنطقة الرطبة
والمسافة البينية بين النقطتين. درست الشفافية المحتثة نفقيا في هذا النظام كبديل عن الشفافية المحتثة
كهرومغناطيسيا. تم السيطرة على التيار النفقي بين النقطتين الكميتين المترابطتين بوساطة فولتية خارجية مسلطة
على النظام. صمم النظام بمعاملات تلائم الشبكات البصرية العاملة ضمن حزمة 100 Gbits/s وقد حصلنا على
عامل ابطاء عالي وكان بمقدار $10^9$. وهذا ملائم في بناء الحواجز البصرية شبه الموصلة من جزيئة نقاط كمية
اذ يمكن السيطرة على ابطاء الضوء من خلال الفولتية المسلطة على النظام.